frontiers | Frontiers in Marine Science

TYPE Original Research
PUBLISHED 09 December 2022
DOI 10.3389/fmars.2022.1005068

OPEN ACCESS

EDITED BY
Brivaela Moriceau,
UMR6539 Laboratoire des Sciences de L'environnement Marin (LEMAR), France

REVIEWED BY
Jun-ichi Kadokawa,
Kagoshima University, Japan
Bernard Moussian,
Université Côte d'Azur, France
Xiangbin Ran,
Ministry of Natural Resources, China

*CORRESPONDENCE
Manuel Maldonado
maldonado@ceab.csic.es

SPECIALTY SECTION
This article was submitted to Marine Biogeochemistry, a section of the journal Frontiers in Marine Science

RECEIVED 27 July 2022
ACCEPTED 16 November 2022
PUBLISHED 09 December 2022

CITATION
Maldonado M, López-Acosta M, Abalde S, Martos I, Ehrlich H and Leynaert A (2022) On the dissolution of sponge silica: Assessing variability and biogeochemical implications. *Front. Mar. Sci.* 9:1005068. doi: 10.3389/fmars.2022.1005068

On the dissolution of sponge silica: Assessing variability and biogeochemical implications

Manuel Maldonado[1]*, María López-Acosta[1,2], Samuel Abalde[1,3], Isabel Martos[1], Hermann Ehrlich[4,5] and Aude Leynaert[6]

[1]Centro de Estudios Avanzados de Blanes (CEAB), CSIC, Blanes, Spain, [2]Instituto de Investigaciones Marinas (IIM), CSIC, Vigo, Spain, [3]Department of Zoology, Swedish Museum of Natural History, Stockholm, Sweden, [4]Institute of Electronic and Sensor Materials, TU Bergakademie Freiberg, Freiberg, Germany, [5]Center for Advanced Technology, Adam Mickiewicz University, Poznan, Poland, [6]Institut Univeresitaire Européen de la Mer. LEMAR UMR, Pluozané, France

The dissolution of the biogenic silica that constitutes the skeletons of silicifying organisms is an important mechanism for regenerating dissolved silicon in the ocean. The silica skeletons deposited to the seafloor after the organisms die keep dissolving until becoming definitively buried. The low dissolution rate of sponge skeletons compared to that of diatom skeletons favors their burial and makes sponges (Phylum Porifera) to function as important silicon sinks in the oceans. However, it remains poorly understood whether the large variety of siliceous skeletons existing in the Porifera involves similar variability in their dissolution rates, which would affect the general conceptualization of these organisms as silicon sinks. Herein we investigated kinetics of silica dissolution for major types of skeletons in the three siliceous lineages of Porifera, following standardized digestion conditions in 1% sodium carbonate with orbital agitation at 85°C. The results are compared with those of a previous study conducted under identical conditions, which considered diatom silica, sponge silica, and lithogenic silica. Unexpectedly, the silica of homoscleromorph sponges dissolved only a bit slower than that of freshly cultured diatoms and as fast as diatom earth. However, the rest of sponge skeletons were far more resistant, although with some differences: the isolated spicules of hexactinellid sponges dissolved slightly faster than when forming frameworks of fused spicules, being hexactinellid frameworks as resistant to dissolution as the silica of demosponges, irrespective of occurring in the form of isolated spicules or frameworks. The experiments also indicated that the complexation of sponge silica with aluminum and with chitin does not increase its resistance to dissolution. Because the rapidly-dissolving homoscleromorph sponges represent less than 1% of extant sponges, the sponge skeletons are still conceptualized as important silicon sinks due to their comparative resistance to dissolution. Yet, the turnover of silica into dissolved silicon will always be faster in environments dominated by hexactinellids with isolated spicules than in environments dominated by other hexactinellids and/or demosponges. We

discuss whether the time required for a given silica type to completely dissolve in 1% sodium carbonate could be a predictor of its preservation ratio in marine sediments.

KEYWORDS

sponge silica, silica turnover, silicate regeneration, sediment digestion, chitin, aluminum, total biogenic silica, silicon cycling

Introduction

In the marine biogeochemical cycle of silicon (Si), siliceous sponges are recognized as distinctive players (Maldonado et al., 2012; Tréguer and De La Rocha, 2013; Tréguer et al., 2021). They are slow consumers compared to diatoms and their main effects are mediated through long-term accumulation of impressive Si standing stocks in the form of silica skeletons in the living populations. Those skeletons are deposited to the sediments once the sponges die. Deposited skeletal pieces feed a fossil record dating back to the Early Cambrian, 525 mya (Tang et al., 2019). More questionable proposals suggest some Precambrian fossil vestiges to be sponge silica skeletons (Muscente et al., 2015). The sponge skeletons accumulated in marine sediments make important local to regional silica reservoirs (Rützler and Macintyre, 1978; Bavestrello et al., 1996; Chu et al., 2011; Gutt et al., 2013; Murillo et al., 2016; Maldonado et al., 2021; López-Acosta et al., 2022). A first quantification of the deposition and burial of sponge skeletons, which occurs more markedly on continental margins and around seamounts, revealed that these processes lead to a substantial Si sink in the global ocean (Maldonado et al., 2019). Burial of sponge silica is favored by its high resistance to dissolution compared to that of the silica of other common marine silicifiers, such as radiolarians and diatoms. For instance, about 45.2% (on average) of the sponge silica deposited to the sediments per year is estimated to become buried permanently (Maldonado et al., 2019), while the ratio for diatom silica is only about 7.5% (Tréguer et al., 2021), being the rest recycled as silicic acid (DSi= dissolved silica) that escapes from the sediments to the bottom water. Thus, the resistance to dissolution of the biogenic silica (BSi) produced by the various marine silicifiers has important implications to the recycling of DSi, which is, in turn, a pivotal nutrient sustaining primary marine productivity (Nelson et al., 1995).

The approximately 9,500 extant species of sponges described taxonomically (de Voogd et al., 2022) are distributed into four major lineages, three of them characterized by having siliceous skeletons: Demospongiae (84%), Hexactinellida (7%), and Homoscleromorpha (1%); sponges with a calcareous skeleton make the remaining 8% of species. Since the 1970's, a variety of experimental studies have consistently concluded that the silica constituting the skeletons of sponges is more resistant to dissolution than diatom silica, in both seawater and alkaline solutions (Kamatani, 1971; Kamatani and Oku, 2000; Maldonado et al., 2005; Chu et al., 2011; Maldonado et al., 2019), for reasons that are not yet well understood. However, a study by Bertolino et al. (2017) proposed that the resistance to dissolution of the silica of some hexactinellid sponges could be not that strong, since relatively large spicules of hexactinellids (particularly those in the family Rosellidae) appeared to dissolve almost entirely in the course of an 8 month experiment. This view was contested by a subsequent study investigating the Si cycle in an aggregation of rosellid hexactinellids (Maldonado et al., 2021), which documented that superficial silica layers of the spicules of rosellid hexactinellids progressively peel off and detach (i.e., silica delamination). Thus, the "high silica dissolution rate" reported by Bertolino et al. (2017) mostly accounted for unnoticed mechanical BSi delamination rather than for actual chemical BSi dissolution. To further investigate the potential differences in the dissolution dynamics of the sponge silica between major sponge lineages, we have conducted the present study. To understand the between-group variability of the dissolution properties of the BSi is important, because such property affects the general conceptualization of siliceous sponges as a relevant Si sink in the global ocean. It also affects the assumptions underlying the quantification of Si cycling through sponges. Thus, we examine herein whether there are marked differences in the resistance to dissolution between different types of siliceous skeletons in the phylum Porifera, by conducting comparative laboratory dissolution experiments based on standard methodology.

Likewise, there is no mechanistic understanding about the reasons of the comparatively high resistance of sponge silica to dissolution. Two main hypotheses have been postulated (Maldonado et al., 2012), but never tested experimentally: 1) the molecular network of the sponge silica would incorporate aluminum (Al) in larger quantities than diatom silica. Aluminum is known to stabilize covalently the silica matrix of diatoms (Machill et al., 2013), lowering its solubility by as much as 25% when one out of every 70 Si atoms is substituted by an Al (III) ion (Van Bennekom et al., 1991; Dixit et al., 2001; Van Cappellen et al., 2002); 2) the spicules of some hexactinellid

sponges are known to incorporate chitin layers intercalated between the concentric silica layers (Ehrlich et al., 2007b; (Ehrlich et al., 2016). Since chitin is a skeletal amino polysaccharide highly resistant to degradation, its presence could hamper the chemical attack to the most accessible sites of the BSi molecular structure, decreasing solubility. These two hypotheses are herein tested experimentally in an attempt to improve our understanding of the processes governing the dissolution and recycling of the sponge silica.

Materials and methods

Digestion of sponge silica

The dissolution kinetics of the skeletal BSi of a variety of sponge species were compared using a 1% solution of sodium carbonate as standard dissolution medium (DeMaster, 1991). Representatives of the main skeletal types in the three phylogenetic lineages of siliceous sponges were selected for the experiment. For the demosponge lineage, we selected 2 skeleton types: 1) millimeters long oxeas and anchor-like spicules (anatriaenes) that are naturally exposed to the seawater because they protrude out of the sponge body to form the rootlets that anchor the sponge *Geodia hentscheli* to the bottom (Figure 1A), 2) pieces of the hypersilicified skeletal framework of fused desmas in the lithistid demosponge *Leiodermatium pfeifferae* (Figure 1B). For the homoscleromorph lineage, we selected the combination of small isolated monaxonic triaxonic, and tetraxonic spicules of the species *Corticium candelabrum* (Figure 1C). For the hexactinellid lineage, we also selected two skeleton types: 1) the skeleton of *Aphrocallistes vastus* (Figure 1D) in which a variety of isolated hexactinal spicules and a massive dictyonal skeletal framework of fused skeletal pieces co-occur; 2) the skeleton of only isolated spicules from the body wall of three rosellids, *Schaudinnia rosea* (Figure 1E), *Asconema setubalense* (Figure 1F), and *Vazella pourtalesii* (Figure 1G). The group of rosellid hexactinellids included 3 species in order to facilitate a within-group assessment of variability in the dissolution rate and compare the results with a previous study suggesting that the resistance to dissolution of the silica of rosellid hexactinellids

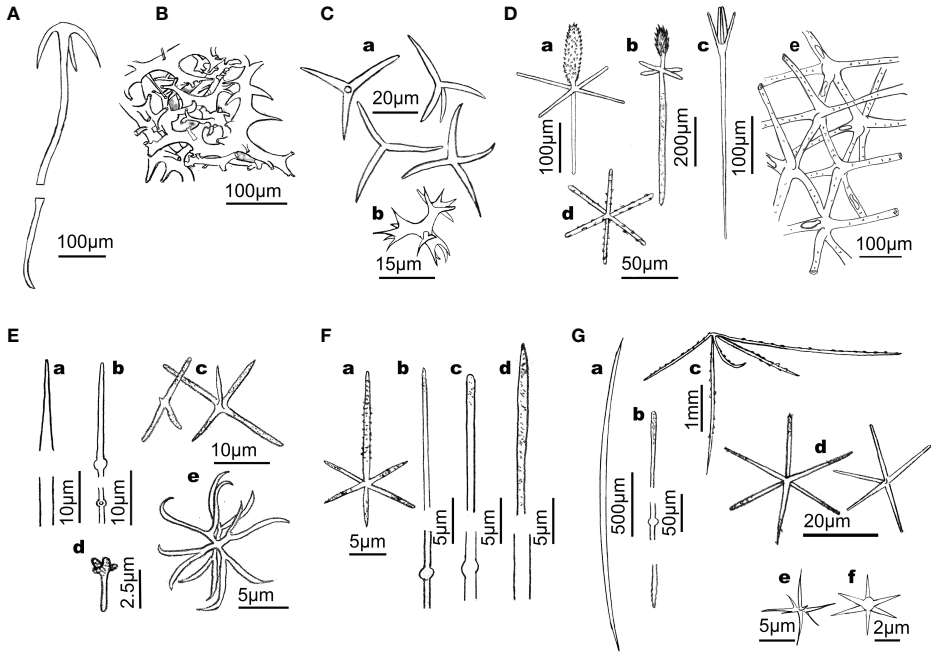

FIGURE 1
Line drawings summarizing the main types of siliceous skeletons involved in the dissolution experiment. **(A)** Anatriaene from the rootlets of the astrophorid demosponge *Geodia hentscheli*. **(B)** Skeletal framework of fused desmas of the lithistid demosponge *Leiodermatium pfeifferae*. **(C)** Microtriactines and microtetractines (a) along with candelabra (b) of the homoscleromorph *Corticium candelabrum*. **(D)** Skeleton of hexactinellid hexactinosid *Aphrocallistes vastus*, where a variety of hexactinal spicules (e.g., a, b: dermal pinnule; c: dermal scopule; d: parenchymal hexactine) and a skeletal dictyonal framework (e) co-occur. **(E)** Skeleton of the hexactinellid rosellid *Schaudinnia rosea*, which lacks skeletal framework and contains, among other skeletal pieces, a variety of diactinal spicules (a, b) within the body wall, dermal triactines and pentactines (c, d), and hexasters (e). **(F)** Skeleton of the hexactinellid rosellid *Asconema setubalense*, containing, among other skeletal pieces, atrial hexactines **(A)** and diactines of several sizes (b–d). **(G)** Skeleton of the hexactinellid rosellid *Vazella pourtalesii*, containing, among other skeletal pieces, diactinal (a, b) and pentactinal (c) spicules that reinforce the body wall and project out of the body, along with smaller pentactines and hexactines (d), and a variety of hexasters (e) and microhexactines (f).

might be much lower than that of other sponges (Bertolino et al., 2017). In addition to the sponge skeletons, we also dissolved aged frustules of diatoms in the form of diatomaceous earth from a Miocene deposit (Castalia diatom earth; https://www.naturitas.es/p/hogar-y-huerto/huerto/abonos-sustratos-y-fertilizantes/tierra-de-diatomeas-250-g-castalia).

Digestions were based on 5 silica subsamples of each skeleton type. Each subsample consisted of ~2.997 mg of acid-cleaned, dried BSi, which is equivalent to ~1.4 mg Si (Supplementary Data File S1). To obtain the silica, pieces of sponge tissue were boiled for a few minutes in concentrated nitric acid, then rinsed in distilled water, and finally in ethanol, prior to dry them to constant weight in an oven to 60°C for several days. Digestions of cleaned BSi were conducted in 50 mL, hermetically-closed Teflon bombs immersed in distilled water at 85°C with orbital agitation, using a 50L SBS TBA-30 bath that was user-modified for agitation and temperature control (Supplementary Video S1). Digestion Teflon bombs were sampled at 0, 2, 3, 4, 5, 6, 8, 12, 24, 48, 60, 72, and 84 h. At each sampling time, 1 mL of digesting solution was pipetted out after gently centrifugation of bombs at 1500 rpm for 3 min. The sampled digesting solution was added to 19 mL of 0.021N HCl solution for buffering and blocking the digestion reaction, bringing the pH of the resulting mix down to 6, an optimal value for colorimetric determination of Si concentration (± 5%) using an Alliance Futura autoanalyzer. Finally, the % of Si released during digestions was plotted against time for depicting between-material differences in dissolution kinetics. Additionally, two spare Teflon tubes from each material were poured on a 0.45 cm polycarbonate filter of 1µm pore at 6h and 24h. The retained particulate BSi material was subsequently coated and examined under a high resolution Jeol Field Emission J1700S SEM (University of Barcelona, Spain).

Results are presented as percentage of dissolved Si over time rather than just mere changes in DSi concentration in the digestion bombs. Unlike the raw values of DSi concentrations, the percentages of dissolved Si overtime incorporate three corrections that make their comparison straightforward, as it follows: 1) At every sampling time, 1mL is extracted from the bombs for analysis. Consequently, the volume is decreasing overtime and the DSi concentration is increasing at a higher pace than it would be expected by mere silica dissolution. 2) Although we used equivalent amounts of Si (approx. 1.4 mg Si) in each sample replicate across materials, the process of weighing always involves a small weight variation (± 1.5%) across samples. Such variation, if not corrected, becomes an additional confounding factor complicating the interpretation of DSi concentrations. 3) Not all sponge silicas have the same purity, due to their different levels of complexation of the silica with organic components (chitin, actin, other proteins embedded in the silica, etc.). The purity levels, which are indicated in the Supplementary Data Files S1, S2, can only be calculated after the 84h digestion. Again, the DSi concentration need to be corrected by this factor to yield the correct percentage of BSi dissolution.

For comparative purposes and to generate a more general pattern for the resistance to dissolution of the various types of sponge BSi, we plotted together the results obtained here and those obtained from an experiment previously conducted under identical experimental conditions by our team and published elsewhere (Maldonado et al., 2019). In that previous study, we processed two additional types of demosponge skeletons: small needle-like (oxea) spicules of *Petrosia ficiformis*, and small star-like spicules (cortical spherasters) of *Chondrilla caribensis*. Frustules of freshly cultured diatoms (*Thalassiosira weissflogii*) were also processed as representative of diatom BSi. Two aluminosilicates (benthonite and kaolinite) were used as representatives of the lithogenic silica (LSi). The only methodological difference between the previous digestion study and the current one is that we used eight replicates per material in the former versus five replicates in the current one. All together, the global comparative analysis included fresh and subfossil diatom skeletons, four types of demosponge skeletons, four types of hexactinellid skeletons, one type of homoscleromorph skeleton, and two aluminosilicates.

In addition, we examined statistically the quantitative differences in the resistance to dissolution between 8 main silica types, according to lineage and previously known dissolution behavior: i) frustules of freshly cultured *T. weissflogii* (labelled as *Thalassiosira* BSi, N= 8), ii) diatom earth (diatomite BSi, N= 8), iii) isolated spicules of the homoscleromorph sponge *C. candelabrum* (Homos BSi; N= 5), iv) isolated, delaminating spicules of hexactinellids (Hexact-iso BSi; N= 15), v) dictyonal frameworks of hexactinellids (Hexact-fus BSi; N= 5), vi) isolated spicules of demosponges (Demosp-iso BSi; N= 21), vii) desma frameworks of lithistid demosponges (Demosp-fus BSi; N= 5), viii) kaolinite and bentonite aluminosilicates (Lithogenic silica; N= 16). We calculated the average dissolution percentage per silica type after 5 h in 1% sodium carbonate at 85°C and examined statistically between-type differences using a one-way ANOVA. A period of 5 h was selected for such comparison, because according to the initial postulates of the 1% sodium carbonate approach designed to estimate total biogenic silica in sediments, nearly all biogenic silica should have been dissolved after 5 h (DeMaster, 1991). However, it was recently demonstrated that the approach underestimates the resistance to dissolution of the sponge silica, which at 5-6 hours only shows incipient to moderate signs of dissolution (Maldonado et al., 2019). Initial non-normal dissolution percentages became normally distributed and homoscedastic after an arcsin-square root transformation prior to the ANOVA. "A posteriori" pairwise comparisons to identify the groups of silica types responsible for the differences followed the Holm-Sidak test.

Aluminum effects on silica dissolution

The content of Al of the skeletal silica was determined in the demosponges *Petrosia ficiformis* (needle-like spicules) and *C. caribensis* (aster-like spicules), and in diatomaceous earth. Then, it was used to interpret differences among the three types of siliceous skeletons in the resistance to dissolution. For Al determination, replicates (1 mg BSi each) of acid-cleaned, dried spicules of *P. ficiformis* and *C. caribensis*, and diatomaceous earth were dissolved in 5 mL of 10% HF. Standard solutions of known concentrations were prepared in the same medium as the samples. Al and Si were determined at the PSO/IUEM (Pôle Spectrométrie Océan, Institut Universitaire Européen de la Mer, Brest, France) by inductively coupled plasma-atomic emission spectrometry (ICP-AES) using a Horiba Jobin Yvon® Ultima 2 spectrometer. Statistically significant differences in the Al : Si ratios of *P.ficiformis* (n=7), *C. caribensis* (n=3), and diatomaceous earth (n=4) were examined using a Kruskal-Wallis one-way ANOVA on ranks followed by a posteriori Dunn's tests, given unequal sampling size and departure from normality. The differences in Al content were assessed versus the dissolution pattern of the three BSi types.

Chitin effects on silica dissolution

To test the role of chitin in the resistance of the sponge BSi to dissolution, acid-cleaned spicules of the hexactinellid sponge *Ijimalophus hawaiicus* (containing 15.3 ± 1.3 µg chitin mg^{-1} BSi; Ehrlich et al., 2016) and the demosponge *Petrosia ficiformis* (lacking chitin; this study) were digested in 1% sodium carbonate and their dissolution kinetics compared. As the assayed spicules of *I. hawaiicus* are the ones making the 30-40 cm long, external stalk that anchors the sponge to the soft bottom (Maldonado et al., 2005), we expected these spicules to have developed special mechanisms (e.g., chitin-silica complexing) to prevent their dissolution when being exposed to a continuous flow of passing-by silicon-desaturated seawater. In contrast, the spicule of *P. ficiformis*, which occur "protected" within the sponge mesohyl, would not need such a defense against dissolution. A comparison of the spicules of *I. hawaiicus* with equivalent spicules from other hexactinellid but lacking chitin would have also been a relevant test. However, such a silica was not available to us when conducting this study.

To determine the presence/absence of chitin in the spicules of *P. ficiformis*, we used three analytical techniques: i) Calcofluor White (CFW) staining, ii) chitinase test, and iii) electrospray ionization mass spectrometry ESI-MS. Calcofluor White (Fluorescent Brightener M2R, Sigma-Aldrich, Taufkirchen, Germany) shows enhanced fluorescence after binding to chitin (Tsurkan et al., 2021). This staining method was applied to purified organic matter obtained after demineralization of *P. ficiformis* spicules. The material was soaked in 0.1 M KOH-glycerine-water solution and few drops of the 0.1% CFW solution were added. This mixture was incubated for 3 h in darkness, washed several times with demineralized water, dried at room temperature and examined using BZ-9000 microscope (Keyence, Osaka, Japan) in both light-microscopy and fluorescent microscopy modes. The highly sensitive CFW staining showed no positive results, indicating the absence of chitin (Supplementary Figure S1). Likewise, the chitinase digestion test (Ehrlich et al., 2010), based on light-microscopy detection of enzymatic dissolution of chitin-containing structures confirmed the absence of chitin. Finally, for the electrospray ionization mass spectrometry ESI-MS, samples obtained after final isolation step were hydrolyzed in 6 M HCl for 24 h at 50°C. After the HCl hydrolysis, samples were filtrated through a 0.4 µm filter and freeze-dried in order to remove excess HCl. The remaining solid was dissolved in water for ESI-MS analysis. D-glucosamine (Sigma-Aldrich, Taufkirchen, Germany) was used as standard. The ESI-MS analytical measurements were performed using an Agilent Technologies 6230 TOF LC/MS spectrometer (Applied Biosystems, Santa Clara, CA, USA). Nitrogen was used as the nebulizing and desolvation gas. Graphs were generated using Origin 8.5 for PC (Originlab Corporation, Northampton, MA, USA). Again, the results of ESI-MS analysis showed the absence of the mass spectrum of d-glucosamine, which should consist of three main signals with mw/z=162, 180 and 359, corresponding respectively to the species [M − H_2O^+ H^+], [M + H^+] and [2 M + H^+]. Together, these results provide strong evidence that the biological material isolated from the spicules of *P. ficiformis* contains no chitin.

To test whether the presence of chitin has an effect on the dissolution rate of the silica, two spicule batches were prepared for each of the two sponge species. One batch was treated with the enzyme chitinase for 72 h, the other batch consisted of chitinase-untreated BSi. As chitin occurs internally between the concentric BSi layers, acid-cleaned spicules were grinded to gross dust to facilitate chitinase to reach the chitin embedded in the silica. Each batch contained 5 replicates of 3 mg BSi each, which were deposited in 2 mL Eppendorf vials. In the vials of one of the batches, 0.8 mL of a chitinase solution (1 mg mL^{-1}) was added, being the mix incubated with gentle orbital agitation at 25°C for 72 h. To avoid that some of the silica-associated chitin could not be broken down because of saturation of the chitinase enzyme over the long incubation period, the added amount of chitinase (1.5 units) was about 27-fold that required to digest the amount of chitin expected within the sponge spicules (i.e., 15.3 ± 1.3 µg chitin per mg BSi). The chitinase solution was prepared by adding dust of *Trichoderma viridae* (Sigma; CAS-No 90001-06-3) to potassium phosphate buffer (pH= 6.1). The other half of the vials were incubated without chitinase, adding just the phosphate buffer solution.

After the incubation with chitinase, we did not quantified how much chitin had exactly been dissolved, because of obvious

difficulties. It was just assumed that most of the chitin exposed at the grinded silica had been degraded and that those differences in chitin abundance should be enough to have an effect on the subsequent silica dissolution rate. After the incubation period, the Eppendorf vials were centrifuged and the incubation medium removed by pipetting. Then, we rinsed in ethanol 96% and centrifuged three more times. The ethanol was finally evaporated at 40 °C and the bottom of the vial containing the sample was cut using a scalpel to be dropped into a 50 mL teflon test tube for digestion in 1% sodium carbonate at 85°C (as indicated in the section "Digestion of sponge silica"). 1mL samples from test tubes were taken at times 2, 3, 4, 5, 6, 8, 12, 24, 36, and 48 h.

Results

Comparative dissolution of sponge silica

The digestion in 1% sodium carbonate at 85°C is a method typically used to estimate the amount of biogenic silica in sediments. For correct functioning, the method needs all biogenic silica be completely dissolved before 5 h. However, our experiment shows that, after 5 h, 6 h and 24 h in treatment, a large amount of undissolved sponge silica still persisted (Figures 2–5; Supplementary Data Files S1, S2). At 5 h, the skeletons of the class Demospongiae had dissolved very little, irrespective of being in the form of the hypersilicified desma framework of *Leiodermatium pfeifferae* (12.5 ± 1.8% dissolution; Figures 2A, 3A–C) or the long, isolated spicules of *Geodia hentscheli* rootlets (9.9 ± 0.7% dissolution; Figures 2A, 3D–F). The silica of the class Hexactinellida dissolved a bit more than that of demosponges, but always less than 40% in 5 h. Specifically, the silica of the hexactinellid with the spicules fused in a dictyonal framework (*Aphrocallistes vastus*: 14.4 ± 1.9%; Figures 2A, 3G–O) dissolved more slowly than that of the three rosellid species with isolated, delaminating spicules (*Vazella pourtalesii:* 37.5 ± 5.9%; *Schaudinnia rosea*: 32.8 ± 3.8%; *Asconema setubalense*: 27.9 ± 1.8). The only sponge silica dissolving substantially (74.4 ± 3.9%) in 5 h was that of the class Homoscleromorpha, a small lineage of siliceous sponges represented in the experiment by the tiny isolated spicules of *Corticium candelabrum*. Yet, a virtually complete dissolution (98.6 ± 4.3%) of the BSi of *C. candelabrum* required at least 24 h in treatment.

A qualitative SEM study of the skeletons after 6 h and 24 h in treatment (Figures 3–5) corroborated the quantitative dissolution data. The desma skeleton of demosponge *L. pfeifferae* was only incipiently dissolved (Figure 3A) at 6 h. Its resistance to dissolution caused that even after 24 h in treatment, many desmas were still poorly dissolved (Figure 3B), with not much etching on their surface (Figure 3C). Likewise, many of the spicules of the rootlets of demosponge *G. henstcheli* remained largely undissolved after both 6 h (Figures 3D, E) and 24 h (Figure 3F). The dictyonal framework of the hexactinellid *A. vastus* showed only incipient digestion at 6h (Figures 3G, H), but extensive digestion of the internal silica occurred at 24 h (Figure 3I). Most of the isolated spicules of this species dissolved faster than its dictyonal framework, with, for instance, hexactines (Figures 3H, I), scopula (Figures 3J, K), and pinnules (Figures 3L, M), showing evident signs of dissolution at 6 h and being completely dissolved in the 24 h sample. However, the tiny asters arrived at 6h with only few dissolution cavities on their surface (Figures 3N, O). After 6 h, the spicules of the three rosellid sponges (Figure 4) were a little bit more dissolved than those of *A. setubalense*. Yet, at 6h many of the diactines of *S. rosea* showed only incipient signs of dissolution at their surface (Figure 4A), with the axial canal being relatively well preserved (Figures 4B, C). However, after 24 h, most of the diactines had extensively dissolved from the inside (Figures 4D–F) and some had also delaminated silica layers (Figure 4G, arrow). However, as it also happened for *A. vastus*, the tiny asters were comparatively resistant to dissolution at both 6 h (Figures 4G, H) and 24 h (Figure 4I). In *A. setubalense*, the hexactines (Figures 4J, K) and diactines (Figures 4J, L) showed obvious signs of dissolution at 6 h. The dissolution was more evident in the hexactines, with both more pronounced etching at the surface (Figure 4K) and inside the tips of the actines (arrows in Figure 4J). In *V. pourtalesii*, a combination of dermal and choanosomal diactines, along with a tiny aster (a), remained all largely undissolved after 6h, with obvious signs of silica delamination, rather than silica digestion (Figure 4M). Likewise, the hexactines of this species remained largely undissolved at 6h (Figure 4N), though with evidence that the most peripheral silica layer (arrows) had been partially dissolved (Figure 4O, arrows). Surprisingly, many of the micro-spicules of *C. candelabrum* were still present after 6h (Figure 5A). However, detailed inspection revealed that those spicules had experienced substantial dissolution at their tips and inside (Figures 5A–C, arrows), as well as on their surface (Figure 5D), showing a surface etching pattern different from that in demosponges and hexactinellids. After 24 h, most of these micro-spicules had been entirely dissolved. Yet, some were still undissolved after 24 h (Figures 5E, F), remaining unclear the reasons for the resistance to dissolution of only some spicules, given than they are similar in shape and structure to their dissolved counterparts.

When previously published data for several kinds of silica digested in 1% sodium carbonate in a fully comparable experimental setup (Maldonado et al., 2019) were plotted together with the data of the current study, a wider context of reference emerges (Figure 2B) to better assess within-group and between-group patterns of sponge silica dissolution. It can be seen that the dissolution of the diatom earth at 5 h (75.4 ± 6.6%) is nearly identical to that of the homoscleromorph sponge *C. candelabrum*, but less than that of freshly cultured diatoms (99.2 ± 2.9%; Figure 2B). It can also be noticed that at 5h, the

10.3389/fmars.2022.1005068

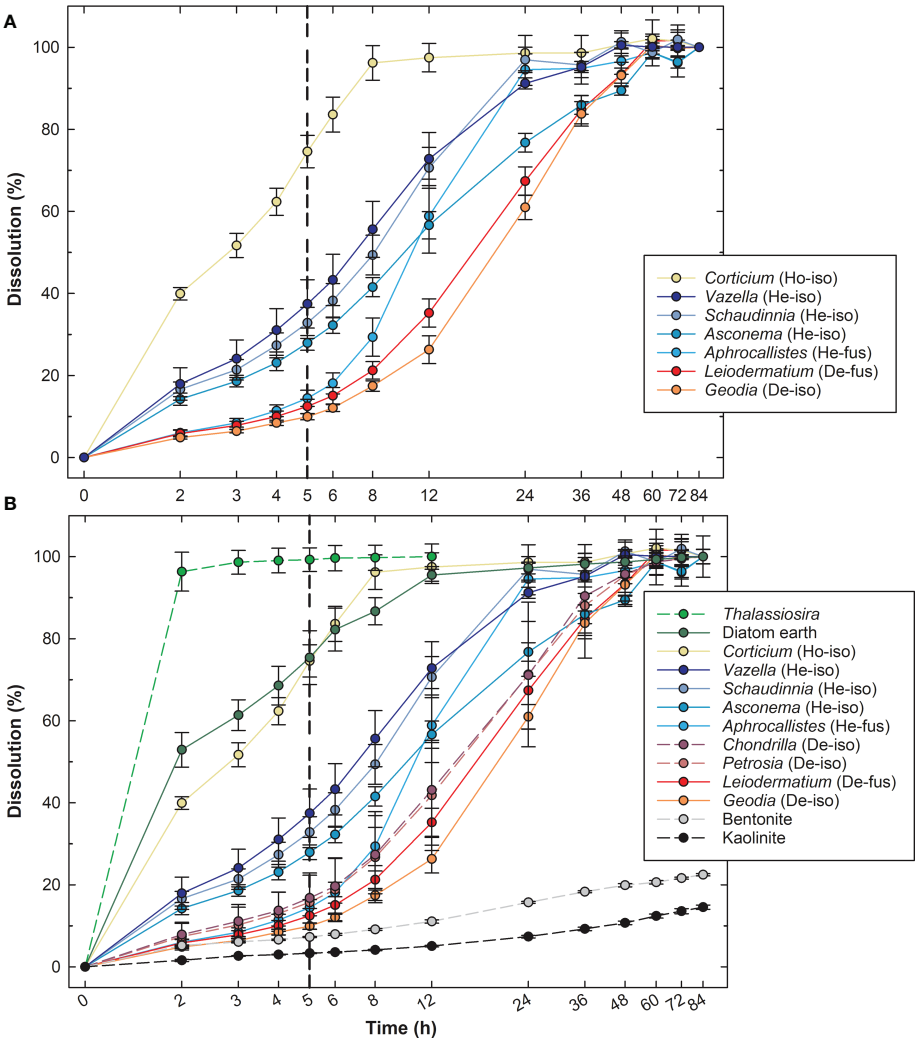

FIGURE 2
Dissolution (%; average ± SD) dynamics of various siliceous materials in 1% sodium carbonate in gentle agitation during 84 h. **(A)** Comparative dissolution of major types of sponge siliceous skeletons assayed in the current study: small isolated spicules of *Corticium candelabrum* in the Class Homoscleroemorpha (Ho-iso); delaminating, isolated spicules of three rosellids species, *Vazella pourtalesii*, *Schaudinnia rosea*, *Asconema setubalense* in the Class Hexactinellida (He-iso); spicules of *Aphocallistes vastus* fused in a dictyonal silica framework (He-fus); desmas of *Leiodermatium pfeifferae* fused in a silica framework in the Class Demospongiae (De-fus); isolated spicules from the rootlets of *Geodia hentscheli* in the Class Demospongiae (De-iso). **(B)** Comparison of the dissolution dynamics of the above described sponge skeleton types in comparison with those of diatom *Thalassiosira weissflogii*, diatom earth, isolated aster-like spicules of demosponge *Chondrilla caribensis* (De-iso), isolated needle-like spicules of desmosponge *Petrosia ficiformis* (De-iso), and aluminosilicates bentonite and kaolinite, as detailed in Maldonado et al. (2019), and herein represented by dashed lines. Note that the representation of the dissolution line of *T. weissflogii* and *C. candelabrum* ends at 12 h and 60 h, respectively, because silica dissolution is virtually completed.

lithogenic silica has dissolved between 3% and 8% on average, the demosponge silica between 9% and 14%, and the hexactinellid silica between 14% and 37%. Differences in the resistance to dissolution were further examined quantitatively (Figure 6) by grouping the various digested materials by main silica type, as it follows: frustules of freshly cultured *T. weissflogii* (*Thalassiosira* BSi), diatom earth (diatomite BSi), isolated spicules of the homoscleromorph sponge *C. candelabrum* (Homos BSi), isolated, delaminating spicules of hexactinellids (Hexact-iso BSi), dictyonal frameworks of hexactinellids (Hexact-fus BSi), isolated spicules of demosponges (Demosp-iso BSi), desma frameworks of lithistid demosponges (Demosp-fus BSi), kaolinite and bentonite aluminosilicates (Lithogenica silica). The one-way ANOVA comparing average dissolution percentage (arcsin-sqroot transformed) per silica type after 5 h hours found significant between-type differences ($F= 380.6$, $P < 0.001$; see extended statistics of analysis in Supplementary Results S1). The "a posteriori" comparisons are graphically

10.3389/fmars.2022.1005068

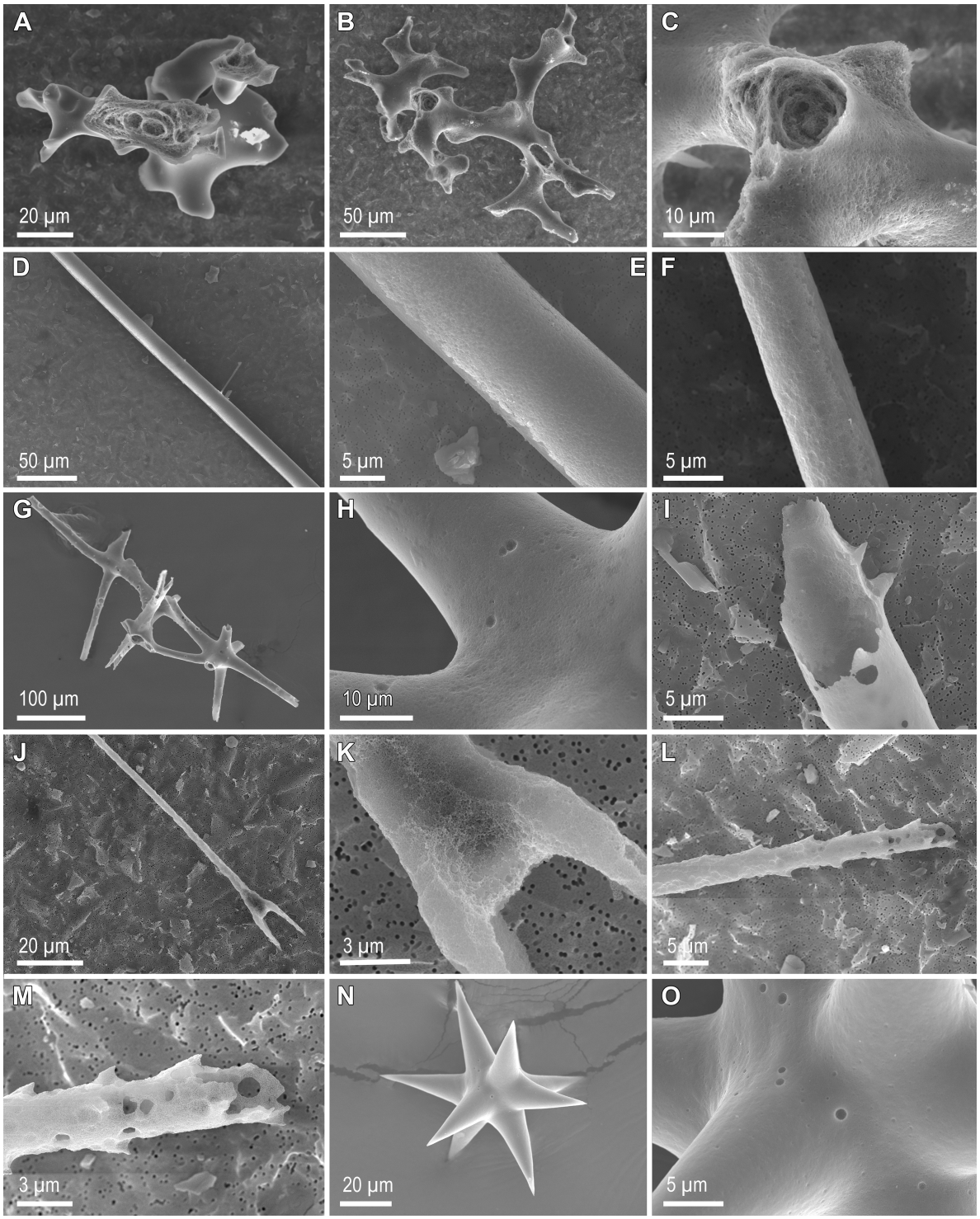

FIGURE 3
Scanning electron microscopy images of sponge skeletal pieces after 6 h and 24 h in 1% sodium carbonate at 85°C. Desmas of demosponge *Leiodermatium pfeffeirae* have largely resisted dissolution after 6 h **(A)** and also after 24 h **(B)**, when only incipient signs of etching at the spicule surface occur **(C)**. Spicules from the rootlets of demosponge *Geodia henstcheli*, which remain largely undissolved and with only incipient etching of their silica surface after 6 h **(D, E)** and 24 h **(F)** in treatment. Dictyonal framework of hexactinellid *Aphrocallistes vastus* remaining largely undissolved after 6 h **(G, H)**, but largely dissolved from the inside after 24 h **(I)**. In contrast to the framework, some of the isolated spicules from *A vastus*, such as the scopula **(J, K)** and the pinnules **(L, M)**, were largely dissolved at 6 h, but other, such as the small asters **(N)**, showed only incipient signs of dissolution at this time **(O)**.

10.3389/fmars.2022.1005068

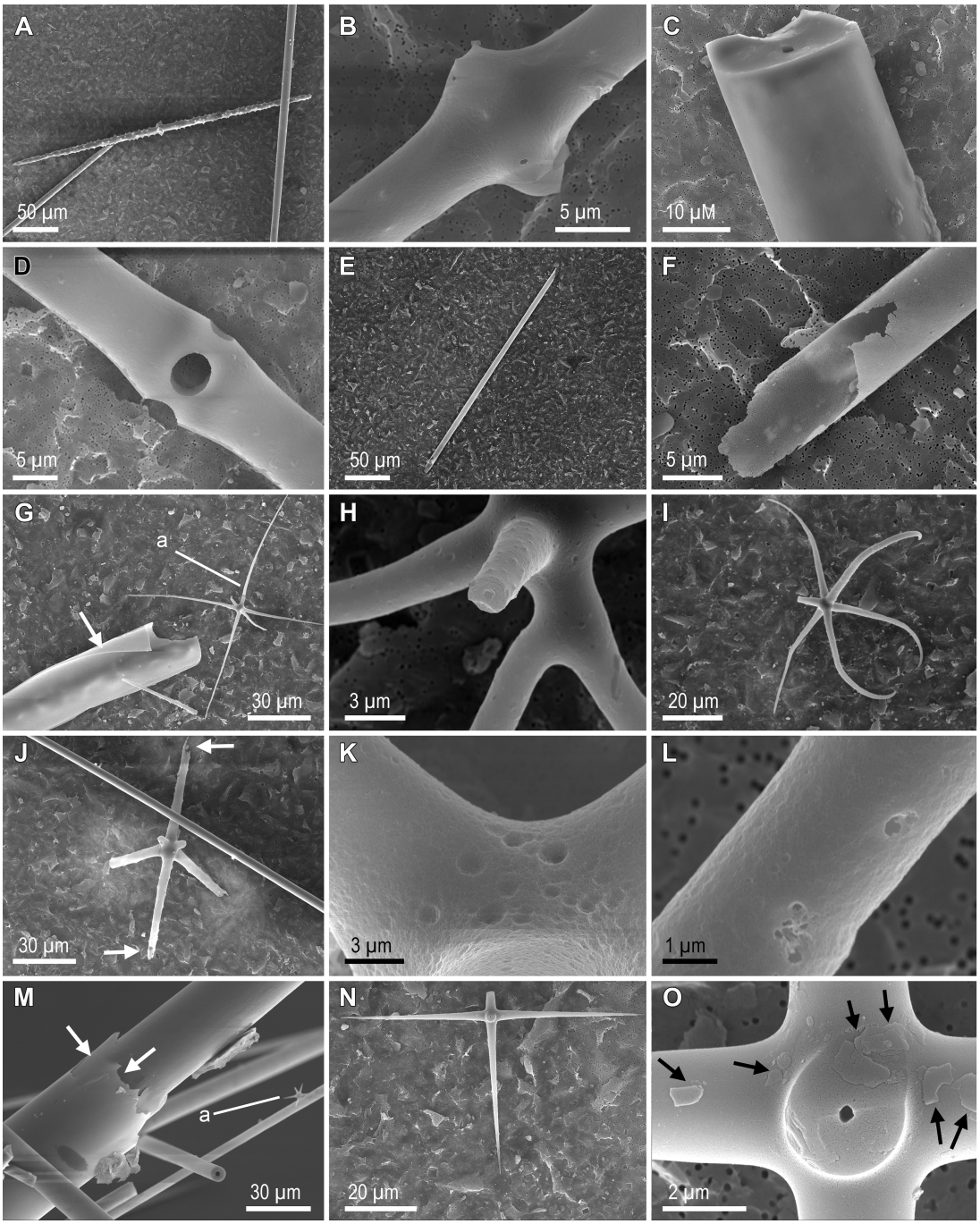

FIGURE 4
Scanning electron microscopy images of sponge skeletal pieces after 6 h and 24 h in 1% sodium carbonate at 85°C. Dermal **(A, B)** and choanosomal **(A, C)** diactines of hexactinellid *Schaudinnia rosea* showing weak dissolution at 6 h, but more extensive dissolution after 24 h **(D–F)**. Unlike the large spicules, the tiny asters **(A)** remained largely un dissolved after both 6h **(G, H)** and 24 h **(I)**. Note in G the occurrence of an undissolved peripheral layer (arrow) delaminated from a large choanosomal diactine. Hexactine **(J, K)** and diactine **(J, L)** of hexactinellid *Asconema setubalense*, showing moderate signs of dissolution at 6 h. The dissolution is more evident in the hexactine, with both more pronounced etching at the surface **(K)** and also inside the tips of the actines (arrows in J). **(M)** A combination of dermal and choanosomal diactines of hexactinellid *Vazella pourtalesii*, along with a tiny aster (a), all remaining largely undissolved after 6 h. Note signs of delamination of the peripheral silica layers (arrows). **(N)** Hexactine of *V. pourtalesii* remaining largely undissolved at 6 h, although with evidence **(O)** that the most peripheral silica layer (arrows) has been partially dissolved.

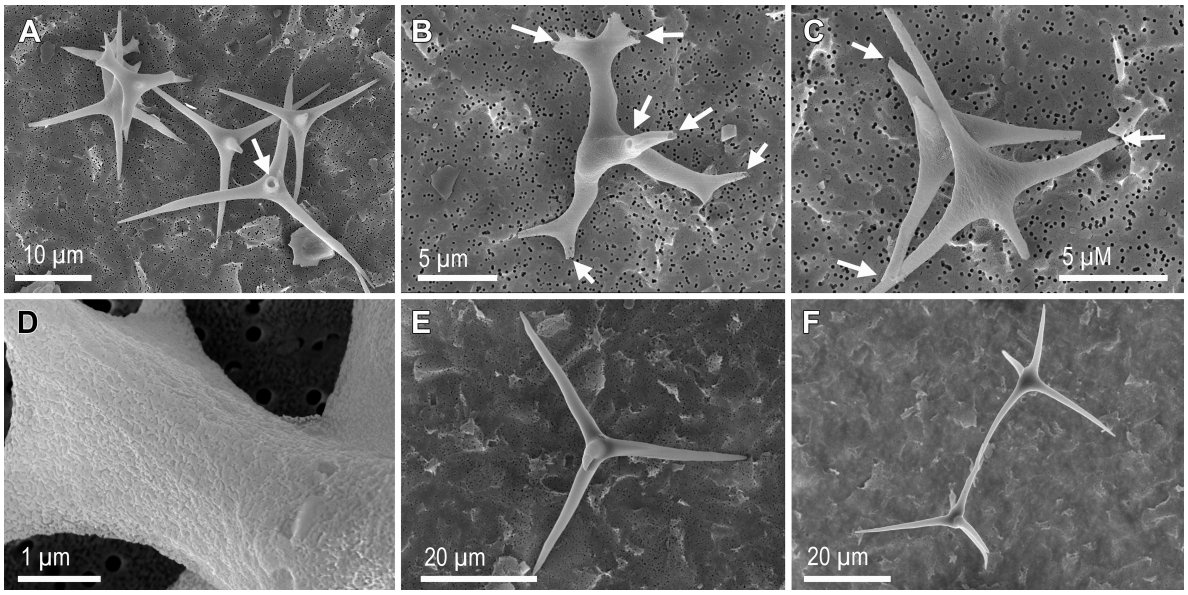

FIGURE 5
Scanning electron microscopy images of sponge skeletal pieces of the homoscleromorph *Corticium candelabrum* after 6 h and 24 h in 1% sodium carbonate at 85°C. Many of the microspicules were still present after 6 h **(A–C)**. However, they all showed substantial dissolution at their tips and inside (arrows), as well as at their surface **(D)**, revealing a surface etching pattern different from that in demosponges and hexactinellids. After 24 h, very few spicules remained undissolved **(E, F)**, being unclear the reasons for the resistance of such few spicules, given than they are similar in shape and structure to their dissolved counterparts.

summarized in Figure 6. They show that fresh frustules (99.3 ± 2.9%), diatomite (75.4 ± 6.6%) and the tiny spicules of homosclerophorid sponges (74.6 ± 3.9%) dissolved at relatively high rates, which —in the conceptual frame of these multiple comparisons— were not significantly different from each other. The isolated, delaminating spicules of rosellid hexactinellids (32.7 ± 5.6%) dissolved significantly slower than the former BSi types, but they still did it about twice faster than the dictyonal frameworks of hexactinellids (14.4 ± 2.0%), the isolated spicules of demosponges (14.8 ± 6.0%), and the desmas frameworks of demosponges (12.5 ± 1.8%), the three of which did not dissolve significantly different from each other. All types of biogenic silica assayed dissolved significantly faster than the lithogenic silica (5.3 ± 2.0%). In terms of magnitude, the most important difference occurs between the group made by diatom frustules (fresh and aged) plus spicules of homoscleromorph sponges (84.3 ± 12.9%) versus the group made by the silica of the remaining sponge skeletons (20.3 ± 10.1%).

Effects of aluminum and chitin on silica dissolution

To test the role of aluminum (Al) in explaining the patterns of resistance to dissolution of the sponge BSi, the spicules of two sponge species (*Chondrilla caribensis* and *Petrosia ficiformis*) and diatomaceous earth were analyzed for their Al/Si atom:atom ratio. The average (± SD) Al/Si ratio in the diatomaceous earth ($2.07x10^{-2} \pm 1.45x\ 10^{-2}$) was significantly higher than those of the two spicules ($1.60x10^{-3} \pm 0.92x10^{-3}$ in *C. caribensis* and $2.65x10^{-3} \pm 1.6x10^{-3}$ in *P. ficiformis*), which in turn were not significantly different from each other (Figure 7 and Supplementary Results S2).

Because the concentration of dissolved Al in most marine environments is very low, the Al/Si ratio in frustules of diatoms either living in the wild or cultured in non-Al-enriched media often falls in the range of 10^{-4} to10^{-3} (Gehlen et al., 2002; Van Cappellen et al., 2002), and we assumed it to be so (not measured) in our cultured diatoms. While the larger Al content of the diatomaceous earth could account for its larger resistance to dissolution relative to freshly cultured diatoms (Figure 2B), it cannot explain the differences in dissolution rate between diatom earth and sponge BSi. The Al/Si ratios of sponge spicules were an order of magnitude smaller than that of diatomaceous earth, but spicules dissolved significantly more slowly (Figure 6). The Al content can neither explain differences in dissolution rate between "types" of sponge silica: the Al/Si ratio in *C. caribensis* is about 1.65 times lower than in *P. ficiformis*, but the dissolution kinetics of both types of sponge skeletons are nearly identical (Figure 2B).

To test whether the presence of chitin increases the resistance to dissolution of the sponge silica, grinded, chitinase-treated and untreated spicules of the hexactinellid

10.3389/fmars.2022.1005068

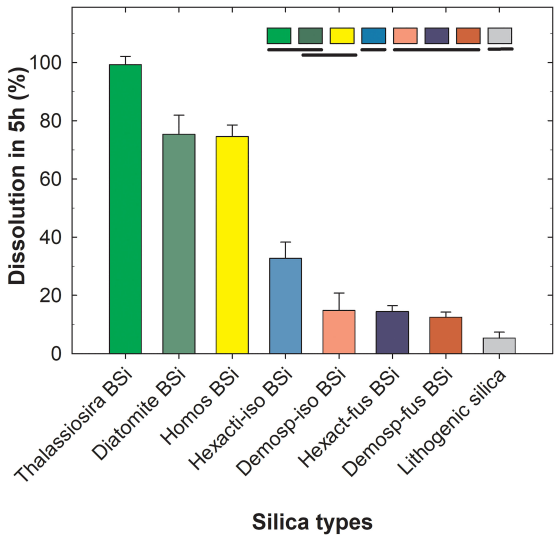

FIGURE 6
Percentage dissolution (avg ± SD) of the various silica types after 5 h in 1% sodium carbonate at 85 °C, ordered in decreasing magnitude: biogeneic silica (BSi) in the form of frustules of diatom *Thalassiosira weissflogii*, diatom earth (diatomite BSi), spicules of homosclerophorid sponge *Corticium candelabrum* (Homos BSi), isolated, delaminating spicules of rosellid hexactinellid sponges (Hexact-iso BSi), isolated spicules of several shapes of demosponges (Demosp-iso BSi), spicules fused in skeletal framework of hexactinellids (Hexact-fus BSi), desmas fused in skeletal framework of demosponges (Demosp-fus BSi), and lithogenic silica represented by aluminosilicates bentonite and kaolinite. A one-way ANOVA detected significant between-type differences in average dissolution (see Supplementary Results S1 for extended statistics). "A posteriori" pairwise comparisons (Holm-Sidak test) are summarized graphically at the top of the graph. Silica types are ordered by decreasing magnitude in average dissolution (%) at 5 h and types that are not statistically different from each other are underlined by the same line. The graph summarizes that fresh frustules, diatomite and spicules of a homoscleromorph sponge dissolve at comparatively higher rates than the rest of assayed BSi, but with no significantly difference from each other. The isolated spicules of hexactinellids dissolve more slowly than the former BSi types, but they still do it two fold faster than the frameworks of fused spicules of hexactinellids, the isolated spicules of demosponges, and the desmas frameworks of demosponges, the three of which do not dissolve differently from each other. All assayed types of biogenic silica dissolved faster than the lithogenic silica.

Ijimalophus hawaiicus (containing chitin) and the demosponge *P. ficiformis* (lacking chitin) were digested in 1% sodium carbonate. Chitinase-treated and untreated replicates of grinded BSi were digested to 100% dissolution, which occurred from 12 h to 24 h (Figure 8), a digestion period shorter than required for entire (not grinded) spicules, which took place in about 60 h (Figure 2B). For both species, dissolution dynamics of chitinase-treated and untreated samples were virtually undistinguishable (Figure 8). Importantly, the silica of *I. hawaiicus* (containing chitin) dissolved even faster during the first 12 h than the silica of *P. ficiformis* (lacking chitin). This pattern is consistent with previous reports that hexactinellid BSi dissolves in seawater faster than demosponge silica (Maldonado et al., 2005; Bertolino et al., 2017). In summary, Al and chitin cannot explain by themselves the distinct resistance to dissolution of the silica of demosponges and hexactinellids.

Discussion

Ecological significance of laboratory dissolution rates

Several compounds, such as sodium carbonate, sodium hydroxide, potassium hydroxide, and hydrofluoric acid, are available for dissolving biogenic silica and extracting it from sediments (Hurd, 1973; Paasche, 1973; Eggimann et al., 1980; Mortlock and Froelich, 1989; Müller and Schneider, 1993; Kamatani and Oku, 2000; Bossert et al., 2019; Maldonado et al., 2019). The most widespread method is the utilization of 1% sodium carbonate (DeMaster, 1981; Conley, 1998). Thus, such a method provides a standardized approach to accurately compare the resistance to dissolution of the main types of sponge BSi skeletons. However, a major challenge remains posed on whether the different dissolution rates in 1% sodium carbonate measured in this study could be translated into some ranking of dissolution rates in the natural environment. To that aim, we are tentatively proposing a simple model that may predict annual dissolution/preservation (%) of the sponge silica relative to its deposition rate to the sediments. Our proposal is here initially formulated after combining some data available in the literature with new data from this study. Though we are aware that our proposal will need additional testing with future data sets, the available arguments for the proposed model are as it follows:

1) The average preservation rate of diatom frustules in sediments (9.2 Tmol y^{-1}) relative to their deposition as silica rain (84 Tmol y^{-1}) is about 10.9% (Tréguer et al., 2021) and such diatom silica is dissolved entirely in 1% sodium carbonate in about 2 h to 3 h (DeMaster, 1991; Figure 2B).
2) In a study of 17 marine sediment cores, the preservation of the sponge silica —in broad sense, that is, combining all spicule types— in marine sediments was estimated at about 45.2 ± 27.4%, relative to its annual deposition (Maldonado et al., 2019). If only the 12 cores dominated by demosponge spicules in that study are considered (i.e., cores 1, 2, 4, 6, 7, 9-15), the average preservation for demosponge skeletons can be recalculated as 46.1 ± 28.4%. The present study shows that such a BSi is completely dissolved in 1% sodium carbonate only after 72 h (Figure 2B).

10.3389/fmars.2022.1005068

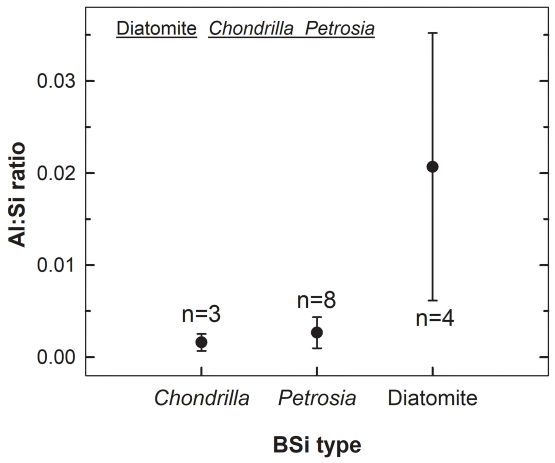

FIGURE 7
Comparison of Al : Si ratios in the BSi of the spicules of the sponges *Chondrilla caribensis* and *Petrosia ficiformis*, and Miocenic diatomaceous earth. A Kruskal-Wallis one-way ANOVA on ranks found significant between-group differences (H= 8.823, *P*= 0.012). The "a posteriori" Dunn's test revealed that the ratio in the diatomaceous earth is significantly larger than that in the spicules of the two sponges (*P*= 0.022, *P*= 0.036), which were not significantly different from each other (*P* > 0.50), as graphically indicated in the upper zone of the graph (i.e., BSi types with Al : Si ratios not significantly different are underlined by the same line). See extended statistics in Supplementary Results S2. "n" refers to the number of replicates analyzed, which varied depending on sample availability.

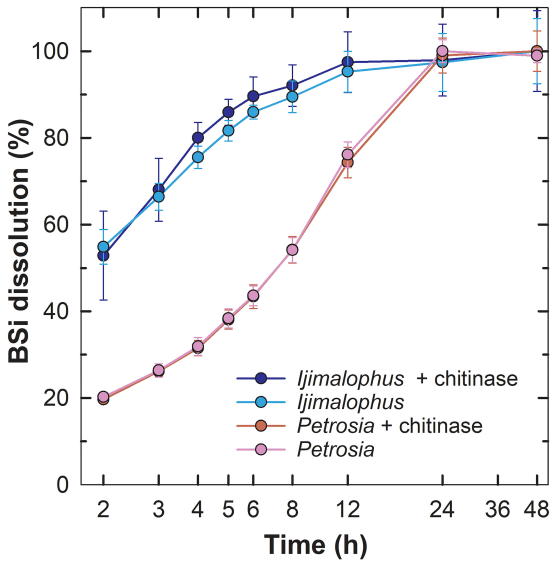

FIGURE 8
Chitinase effects on sponge BSi dissolution. Dissolution kinetics in 1% sodium carbonatate of grinded chitinase-treated and untreated spicules of the hexactinellid *Ijimalophus hawaiicus* and the demosponge *Petrosia ficiformis*. Time (h) is presented in logarithmic scale.

3) The study of sediments in an aggregation of the rosellid hexactinellid *Vazella pourtalesii* estimated that sponge silica preservation by burial relative to its annual deposition rate is about 35.1 ± 10.1% (Maldonado et al., 2021). Such a silica is completely dissolved in 1% sodium carbonate after 48 h (Figure 2B).

When these three datasets are plotted (Figure 9), the model best fitting the relationship between BSi preservation (% relative to deposition) in the sediments and time (h) to total BSi dissolution in 1% sodium carbonate is a linear regression $Y = y_0 + (a \times X)$ (Supplementary Results S3). Such a regression predicts the silica of homosclerophorid spicules to have a comparatively poor average preservation in marine sediments of 22.12 ± 1.38% (Figure 6). Indeed, such a predicted poor preservation is consistent with the rapid dissolution in 1% sodium carbonate detected for the spicules of *C. candelabrum* (Figures 2A, 5). The comparatively rapid dissolution of these spicules may also be the reason why the fossil record of the class Homoscleromorpha is surprisingly poor (Botting and Muir, 2018).

Thus, the proposed model may provide a tentative proxy to estimate natural BSi preservation as a function of time to total dissolution in 1% sodium carbonate. If so, it would save considerable amounts of time in sediment analyses. Yet, a general applicability of this tentative proposal needs to be corroborated in future studies incorporating additional types of BSi, such as radiolarians, benthic diatoms, choanoflagellates, etc. Conducting a dissolution process based on continuous monitoring (e.g., Barão et al., 2015) rather than monitoring at given time steps would also increase accuracy when further testing and/or refining this proxy.

Dissolution patterns and their causes

A mechanistic understanding on how biogenic silica dissolves has proven elusive because the amorphous organic nature of such silica lacks structural order and prevents application of classical techniques used for crystals (Dove et al., 2008). Regarding the BSi of sponges, the experiments indicate that the silica of homoscleromorph sponges dissolved significantly faster than that of the other sponges, following a pattern nearly identical to that of the aged silica of diatom earth. The homoscleromorphs make a small class of sponges, which harbors only nine taxonomic genera and 118 species, that is, it represents less than 1% of extant sponge species. A few of those species (i.e., 21 spp.) do not even have a siliceous skeleton. Therefore, although these sponges may be common at some specific shallow-water tropical and subtropical habitats (typically coral reefs and caves), the magnitude of their global contribution to the Si fluxes in sediments is expected to be negligible.

10.3389/fmars.2022.1005068

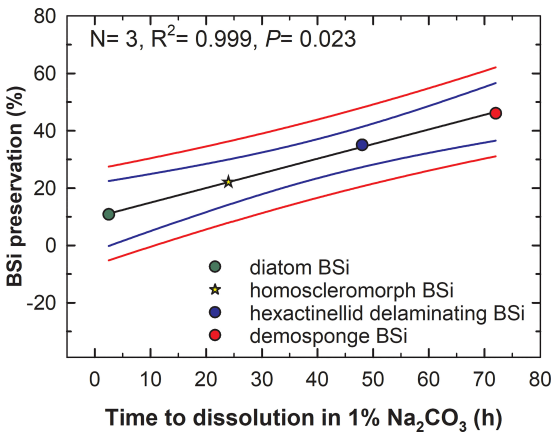

FIGURE 9
Relationship between the time (h) required by the various types of BSi (diatoms, rosellid hexactinellids, demosponges) to dissolve completely in 1% sodium carbonate at 85°C and their respective preservation (%) in the marine sediments. The relationship is best fitted by a linear regression model (black line) in the form of "Preservation (%) = 10.04 + (0.5×dissolution time)", which is statistically significant (see extended statistics in Supplementary Results S3). Blue and red lines indicate the 95% confidence band and the 95% prediction band of model, respectively. The preservation of the silica of homoscleromorph sponges relative to its deposition is predicted to be around 22.12 ± 1.38% (yellow start) as a function of its resistance to dissolution in sodium carbonate (Figure 2).

In contrast to homosclerophorids, the demosponges make the bulk of the sponge fauna on continental shelves, showing also great abundance at bathyal depths. The skeletons of demosponges are found in abundance in sediments from continental margins and around seamounts (Bavestrello et al., 1996; Bertolino et al., 2012; Murillo et al., 2016; Maldonado et al., 2019; Costa et al., 2021). Our results agree with the general notion that the skeletal pieces of demosponges are relatively resistant to dissolution in seawater and alkaline digesters. For instance, (Kamatani 1971), using siliceous spicules of an unidentified demosponge, demonstrated that the spicules dissolved only 0.3% after 24 days in seawater, while the frustules of *Thalassiosira decipiens* did it in 90.1%. Kamatani also reported that appreciable differences occurred between sponge spicules and diatom frustules that were not geologically aged regarding the infra-red spectra of their silica, both in the absorption pattern near 980 cm^{-1} and the ratio of absorption intensities (D2/D1 and D3/D1). Consequently, Kamatani concluded that it "seemed reasonable to assume that the difference in solubility between diatom and sponge silica would be due not only to the thickness and specific surface area, but also to the internal structure suggested by the infra-red spectrum". Thirty years later, (Kamatani and Oku, 2000) reported again large differences in dissolution between the silica of an unidentified demosponge and the silica of the diatoms *Skeletonema costatum* and *Rhizosolenia hebetata* in both NaOH and Na_2CO_3 solutions. In 2005, an 8-month dissolution experiment in sterile seawater reported that needle-like spicules of the hexactinellid *Ijimalophus hawaiicus* dissolved 5%, while dissolution of needle-like and aster-like spicules of demosponges *Petrosia ficiformis* and *Chondrilla caribensis*, respectively, was undetectable (Maldonado et al., 2005). The experiments by Kamatani (1971) along with those by (Maldonado et al., 2005; Maldonado et al., 2019) also provide strong support to the idea that differences in specific surface area are not a major responsible for the comparative resistance of the sponge silica to dissolution. Spicules with drastically different surface areas dissolve at similar slow rates. In some cases, the shapes expected to have lower surface area dissolve even more rapidly than the ones with higher specific surface area, in a clear demonstration that the specific surface area is not a major driver of the differences in the resistance to dissolution between the different types of sponge silica. For instance, the 30µm, star-like sterrasters of the demosponge *Geodia* dissolve more slowly than the 50-cm long, needle-like spicules of the hexactinellid *Ijimalophus* (Maldonado et al., 2005). However, the opposite pattern would be expected if specific surface area was the main responsible for the resistance to dissolution in these sponge silicas. Likewise, the 30µm, star-like oxyasters of the demosponge *Chondrilla* dissolve at identical rate than the 150 µm long, needle-like oxeas of the demosponge *Petrosia* (Figure 2B), despite large predicted differences in their specific surface area.

Sediment studies also provide indirect evidence of the high resistance of sponge silica to dissolution. Extant aggregations of *Geodia* spp. are known to have built a continuous reservoir of well-preserved, aster-like spicules (sterrasters) in the sediments, dating 130,000 years BP (Murillo et al., 2016). In agreement with such a long-term preservation of *Geodia* sterrasters, our experiments indicate that spicules of *Geodia hentscheli* (Figures 2, 3D–F) are among the most resistant to dissolution. It appears that in the many cases in which the function of the sponge skeletons requires direct exposure of the silica to the seawater (e.g., spicules of the attachment rootlets of *G. hentcheli*), mechanisms have been developed through evolution to avoid dissolution and preserve spicule functionality. A paradigmatic example would be the giant siliceous spicule of the hexactinellid *Monorhaphis chuni* that serves as anchoring stalk for the sponge during more than 15,000 years (Jochum et al., 2017), while showing no evident external signs of dissolution during that long period. It remains unclear which are the mechanisms that prevent or slow down sponge silica dissolution, but the Al and chitin contents of the silica do not appear to be major drivers of such a resistance (Figures 7, 8).

Initially, we hypothesized that complexation of the sponge silica with chitin could be a factor slowing dissolution, but it appears to be the opposite, according to our experimental results (Figure 8). To date, chitin has been identified in a variety of 21 marine and three fresh-water sponge species (Talevski et al.,

2020), though rarely incorporated into the silica. It occurs incorporated into the silica of only some hexactinellid sponges (Ehrlich and Worch, 2007; Ehrlich et al., 2007a; Elrich et al., 2008; Tabachnick et al., 2011; Elrich et al., 2016), but it has never been found in the silica of demosponges and homoscleromorphs to date. The microscopic organization of the silica of the hexactinellid *I. hawaiicus*, which contains chitin and dissolves comparatively faster than the chitin-lacking silica of the demosponge *P. ficiformis*, comes into some general agreement with the organization of the silica of the other skeleton type experiencing relative fast dissolution, the spicules of the homosclerophorid *C. candelabrum*. Transmission electron microscopy revealed occurrence of relative thick layers of organic components (of undetermined nature) between the silica layers (Maldonado and Riesgo, 2007). Thus, it appears that complexation with organic materials makes the silica matrix less dense and it could explain the comparatively rapid dissolution detected in homosclerophorids and hexactinellids with delaminating spicules. It is likely that, in the sponge skeletons with a marked concentric layering of the silica due to intercalation sheets of chitin, collagen or other organic compounds, the alkaline digesters may infiltrate more easily between the concentric silica layers, multiplying the surface area exposed to digestion and accelerating the process, relative to other types of sponge silica where silica layers are closely fused to each other. This general pattern may also held at some point for diatom silica, since some experiments have suggested that dissolved protease from environmental bacteria appear to digest by enzymatic hydrolysis some of the proteins embedded in the silica matrix, accelerating the dissolution of the frustules (Roubeix et al., 2008). This effect would be different from the better known hydrolytic attack to the exopolysaccharides and other organic layers that externally cover the frustules of diatoms and that avoid a direct contact with the seawater that otherwise would cause their rapid dissolution (Bidle and Azam, 1999; Toullec and Moriceau, 2018). Such external organic covers have never been reported from sponge silica, despite most sponges having part of their spicules directly exposed to the seawater and despite those spicules not dissolving during the lifetime of the sponges. Thus, the effects of the external organic layer on the dissolution of diatom silica are not directly comparable to the effect of the organic components truly embedded within the silica matrix of the sponge spicules (Maldonado and Riesgo, 2007; Ehrlich et al., 2016).

We also hypothesized that incorporation of Al within the silica matrix could be other of the mechanisms responsible for the slow dissolution of the sponge silica. However, the Al/Si ratios in the sponge silica were an order of magnitude smaller than in diatomaceous earth (Figure 7), but still the sponge spicules dissolved more slowly (Figure 2B). The Al content can neither explain differences in dissolution rate between "types" of sponge silica: the Al/Si ratio in *C. caribensis* was about 1.75 times lower than in *P. ficiformis* (Figure 7), but their dissolution kinetics in the 1% Na_2CO_3 solution were extremely similar (Figure 2B). The effects of other elements (e.g., incorporation of Ge and/or Zn: Sim-Smith et al., 2017; leaching effect of Na^+, K^+, Li^+ ions: Crundwell, 2017) in the general control of BSi dissolution rate need to be addressed in future studies. In the case of spicules that are continuously exposed to seawater to accomplish their ecological function, it cannot be discarded physico-chemical mechanisms — which remain elusive— to favor values of surface free energy that may increase passivation of the external surface of silica to solvents.

Before we can reach a mechanistic understanding of the dissolution of biogenic silica, further characterization of the BSi behavior in seawater and Si-desaturated solutions rich in ions is required. Likewise, a recent surprising report of actin deeply embedded in the silica of demosponges and hexactinellids (Ehrlich et al., 2022) emphasizes the need of deepening into the atom-level characterization of the complexation of BSi with organic elements, which may significantly determine dissolution patterns. The persisting lack of knowledge in this sense is relevant because the dissolution kinetics of the biogenic silica reservoirs in the water column and the sediments are one of the main controls of the biogeochemical cycling of silicon in the ocean.

Conclusions

The main conclusions of this study are several. First, the dissolution properties of the biogenic silica vary not only across organismal phyla, but also within sponges, where differences occur between the main siliceous lineages (i. e., Demospongiae, Hexactinellida, Homoscleromorpha). Second, the bulk of sponge silica still dissolves very slowly compared to diatom silica, except for the microspicules of homosclerophorid sponges. Third, the complexation of the sponge silica with aluminum and chitin does not explain the comparatively higher resistance to dissolution of sponge silica. The intercalation of chitin or other organic elements between concentric silica layers in some hexactinellid and homoscleromorph sponges, if any, facilitates spicule dissolution rather than preventing it. Fourth, the spicules of hexactinellids in the family Rosellidae, which drop off their peripheral silica layers, dissolve about twice faster than the silica of the rest of hexactinellids and demosponges, but still substantially slower than diatom skeletons. Fifth, a chemical digestion of sediments rich in sponge spicules is little appropriate to obtain accurate determinations of total BSi in them, due to large differences in resistance to dissolution between the various types of biogenic silica. Sixth, developing a methodology to easily quantify the amount of sponge silica and its preservation in marine sediments remains as a major future challenge. Seventh, we propose herein a tentative proxy to be

further explored, suggesting that preservation of sponge silica in marine sediments may be grossly estimated as a function of time to its total dissolution in 1% sodium carbonate.

Data availability statement

The original contributions presented in the study are included in the article/Supplementary Material. Further inquiries can be directed to the corresponding author.

Author contributions

MM designed the study and wrote the first manuscript version. Dissolution experiments were conducted by MM, SA, ML-A, and AL. AL analyzed Al contents. HE analyzed chitin contents. MM and IM conducted the SEM study. All authors contributed to the article and approved the submitted version.

Funding

This research has been funded by projects "Dark-Si" (Spanish Ministry of Science, Innovation and Universities: PID2019-108627RB-I00) and "SIFS" (Spanish Council for Scientific Research: PIE-202130E034) awarded to MM. HE was partially supported by OPUS 19 grant from the National Science Centre, Poland (2020/37/B/ST5/01909) and by Alexander von Humboldt Polish Honorary Research Scholarship (FNP, Poland).

Acknowledgments

Celia Sitjá, Erik García, and Marta García are thanked for helping at different steps of the experiments, Morgane Galliniari for conducting ICP-AES analyses, and Maravillas Abad for autoanalyzer silicate determinations.

Conflict of interest

The authors declare that the research was conducted in the absence of any commercial or financial relationships that could be construed as a potential conflict of interest.

Publisher's note

All claims expressed in this article are solely those of the authors and do not necessarily represent those of their affiliated organizations, or those of the publisher, the editors and the reviewers. Any product that may be evaluated in this article, or claim that may be made by its manufacturer, is not guaranteed or endorsed by the publisher.

Supplementary material

The Supplementary Material for this article can be found online at: https://www.frontiersin.org/articles/10.3389/fmars.2022.1005068/full#supplementary-material

References

Barão, L., Vandevenne, F., Clymans, W., Frings, P., Ragueneau, O., Meire, P., et al. (2015). Alkaline-extractable silicon from land to ocean: A challenge for biogenic silicon determination. *Limnol. Oceanogr. Methods* 13, 329–344. doi: 10.1002/LOM3.10028

Bavestrello, G., Cattaneo-Vietti, R., Cerrano, C., Cerutti, S., and Sarà, M. (1996). Contribution of sponge spicules to the composition of biogenic silica in the ligurian Sea. *Pubbl. della Stn. Zool. di Napoli Mar. Ecol.* 17, 41–50. doi: 10.1111/j.1439-0485.1996.tb00488.x

Bertolino, M., Calcinai, B., Capellacci, S., Cerrano, C., Lafratta, A., Pansini, M., et al. (2012). *Posidonia oceanica* meadows as sponge spicule traps. *Ital. J. Zool.* 79, 231–238. doi: 10.1080/11250003.2011.614641

Bertolino, M., Cattaneo-Vietti, R., Pansini, M., Santini, C., and Bavestrello, G. (2017). Siliceous sponge spicule dissolution: In field experimental evidences from temperate and tropical waters. *Estuar. Coast. Shelf Sci.* 184, 46–53. doi: 10.1016/j.ecss.2016.10.044

Bidle, K. D., and Azam, F. (1999). Accelerated dissolution of diatom silica by marine bacterial assemblages. *Nature* 397, 508–512. doi: 10.1038/17351

Bossert, D., Urban, D. A., Maceroni, M., Ackermann-Hirschi, L., Haeni, L., Yajan, P., et al. (2019). A hydrofluoric acid-free method to dissolve and quantify silica nanoparticles in aqueous and solid matrices. *Sci. Rep. 2019 91* 9, 1–12. doi: 10.1038/s41598-019-44128-z

Botting, J. P., and Muir, L. A. (2018). Early sponge evolution: A review and phylogenetic framework. *Palaeoworld* 27, 1–29. doi: 10.1016/J.PALWOR.2017.07.001

Chu, J. W. F., Maldonado, M., Yahel, G., and Leys, S. P. (2011). Glass sponge reefs as a silicon sink. *Mar. Ecol. Prog. Ser.* 441, 1–14. doi: 10.3354/meps09381

Conley, D. J. (1998). An interlaboratory comparison for the measurements of biogenic silica in sediments. *Mar. Chem.* 63, 39–48.

Costa, G., Bavestrello, G., Cattaneo-Vietti, R., Dela Pierre, F., Lozar, F., Natalicchio, M., et al. (2021). Palaeoenvironmental significance of sponge spicules in pre-messinian crisis sediments, northern Italy. *Facies* 67, 9. doi: 10.1007/s10347-020-00619-4

Crundwell, F. K. (2017). On the mechanism of the dissolution of quartz and silica in aqueous solutions. *ACS Omega* 2, 1116–1127. doi: 10.1021/acsomega.7b00019

DeMaster, D. J. (1981). The supply and accumulation of silica in the marine environment. *Geochim. Cosmochim. Acta* 45, 1715–1732. doi: 10.1016/0016-7037(81)90006-5

DeMaster, D. J. (1991). "Measuring biogenic silica in marine sediments and suspended matter," in *Marine particles: Analysis and characterization*, vol. 363–367 . Eds. D. C. Hurd and D. W. Spenser (Washington: American Geophysical Union).

de Voogd, N. J., Alvarez, B., Boury-Esnault, N., Carballo, J. L., Cárdenas, P., Díaz, M.-C., et al. (2022) *World Porifera database*. Available at: https://www.marinespecies.org/porifera/.

Dixit, S., Van Cappellen, P., and van Bennekom, A. J. (2001). Processes controlling solubility of biogenic silica and pore water build-up of silicic acid in marine sediments. *Mar. Chem.* 73, 333–352. doi: 10.1016/S0304-4203(00)00118-3

Dove, P. M., Han, N., Wallace, A. F., and De Yoreo, J. J. (2008). Kinetics of amorphous silica dissolution and the paradox of the silica polymorphs. *Proc. Natl. Acad. Sci. U. S. A.* 105, 9903–9908. doi: 10.1073/PNAS.0803798105/ASSET/8D42F9F4-68B8-421C-AA9E-BF0BC38C3C8D/ASSETS/GRAPHIC/ZPQ9990836760004.JPEG

Eggimann, D. W., Manheim, F. T., and Betzer, P. R. (1980). Dissolution and analysis of amorphous silica in marine sediments. *J. Sediment. Petrol.* 50, 215–225. doi: 10.1306/212F79AF-2B24-11D7-8648000102C1865D

Ehrlich, H., Ilan, M., Maldonado, M., Muricy, G., Bavestrello, G., Kljajic, Z., et al. (2010). Three-dimensional chitin-based scaffolds from verongida sponges (Demospongiae: Porifera). part i. isolation and identification of chitin. *Int. J. Biol. Macromol.* 47, 132–140. doi: 10.1016/j.ijbiomac.2010.05.007

Ehrlich, H., Janussen, D., Simon, P., Bazhenov, V. V., Shapkin, N. P., Erler, C., et al. (2008). Nanostructural organization of naturally occurring composites-part II: Silica-chitin-based biocomposites. *J. Nanomater.* 2008, 1-18. doi: 10.1155/2008/670235

Ehrlich, H., Krautter, M., Hanke, T., Simon, P., Knieb, C., Heinemann, S., et al. (2007a). First evidence of the presence of chitin in skeletons of marine sponges. part II. glass sponges (Hexactinellida: Porifera). *J. Exp. Zool. Part B Mol. Dev. Evol.* 308, 473–483. doi: 10.1002/jez.b.21174

Ehrlich, H., Luczak, M., Ziganshin, R., Mikšík, I., Wysokowski, M., Simon, P., et al. (2022). Arrested in lass: Actin within sophisticated architectures of biosilica in sponges. *Adv. Sci.*, 9 (11), 2105059. doi: 10.1002/advs.202105059

Ehrlich, H., Maldonado, M., Parker, A. R., Kulchin, Y. N., Schilling, J., Köhler, B., et al. (2016). Supercontinuum generation in naturally occurring glass sponges spicules. *Adv. Opt. Mater.* 4, 1608–1613. doi: 10.1002/adom.201600454

Ehrlich, H., Maldonado, M., Spindler, K.-D. D., Eckert, C., Hanke, T., Born, R., et al. (2007b). Evidence of chitin as a component of the skeletal fibers of marine sponges. part i. verongidae (Demospongiae: Porifera). *J. Exp. Zool. (Molecular Dev. Evol.* 308B, 347–356. doi: 10.1002/jez.b.21156

Ehrlich, H., and Worch, H. (2007). "Sponges as natural composites: from biomimetic potential to development of new biomaterials," in *Porifera Research. biodiversity, innovation and sustainability*. Eds. M. R. Custódio, G. Lôbo-Hajdu, E. Hajdu and G. Muricy (Rio de Janeiro: Rio de Janeiro: Museu Nacional), 303–312.

Gehlen, M., Beck, L., Calas, G., Flank, A. M., Van Bennekom, A. J., and Van Beusekom, J. E. E. (2002). Unraveling the atomic structure of biogenic silica: Evidence of the structural association of Al and Si in diatom frustules. *Geochim. Cosmochim. Acta* 66, 1601–1609. doi: 10.1016/S0016-7037(01)00877-8

Gutt, J., Böhmer, A., and Dimmler, W. (2013). Antarctic Sponge spicule mats shape macrobenthic diversity and act as a silicon trap. *Mar. Ecol. Prog. Ser.* 480, 57–71. doi: 10.3354/meps10226

Hurd, D. C. (1973). Interactions of biogenic opal, sediment and seawater in the central equatorial pacific. *Geochim. Cosmochim. Acta* 37, 2257–2282. doi: 10.1016/0016-7037(73)90103-8

Jochum, K. P., Schuessler, J. A., Wang, X.-H., Stoll, B., Weis, U., Müller, W. E. G., et al. (2017). Whole-ocean changes in silica and Ge/Si ratios during the last deglacial deduced from long-lived giant glass sponges. *Geophys. Res. Lett.* 44, 11555–11564. doi: 10.1002/2017gl073897

Kamatani, A. (1971). Physical and chemical characteristics of biogenous silica. *Mar. Biol.* 8, 89–95. doi: 10.1007/BF00350922

Kamatani, A., and Oku, O. (2000). Measuring biogenic silica in marine sediments. *Mar. Chem.* 68, 219–229. doi: 10.1016/S0304-4203(99)00079-1

López-Acosta, M., Maldonado, M., Grall, J., Ehrhold, A., Sitjà, C., Galobart, C., et al. (2022). Sponge contribution to the silicon cycle of a diatom-rich shallow bay. *Limnol. Oceanogr.* 67, 2431–2447. doi: 10.1002/LNO.12211

Machill, S., Kohler, L., Ueberlein, S., Hedrich, R., Kunaschk, M., Paasch, S., et al. (2013). Analytical studies on the incorporation of aluminium in the cell walls of the marine diatom stephanopyxis turris. *BioMetals* 26, 141–150. doi: 10.1007/s10534-012-9601-3

Maldonado, M., Beazley, L., López-Acosta, M., Kenchington, E., Casault, B., Hanz, U., et al. (2021). Massive silicon utilization facilitated by a benthic-pelagic coupled feedback sustains deep-sea sponge aggregations. *Limnol. Oceanogr.* 66, 366–391. doi: 10.1002/lno.11610

Maldonado, M., Carmona, M. C., Velásquez, Z., Puig, A., Cruzado, A., López, A., et al. (2005). Siliceous sponges as a silicon sink: An overlooked aspect of benthopelagic coupling in the marine silicon cycle. *Limnol. Oceanogr.* 50, 799–809. doi: 10.4319/lo.2005.50.3.0799

Maldonado, M., López-Acosta, M., Sitjà, C., García-Puig, M., Galobart, C., Ercilla, G., et al. (2019). Sponge skeletons as an important sink of silicon in the global oceans. *Nat. Geosci.* 12, 815–822. doi: 10.1038/s41561-019-0430-7

Maldonado, M., Ribes, M., and van Duyl, F. C. (2012). Nutrient fluxes through sponges. biology, budgets, and ecological implications. *Adv. Mar. Biol.* 62, 113–182. doi: 10.1016/B978-0-12-394283-8.00003-5

Maldonado, M., and Riesgo, A. (2007). Intra-epithelial spicules in a homosclerophorid sponge. *Cell Tissue Res.* 328, 639–650. doi: 10.1007/s00441-007-0385-7

Mortlock, R. A., and Froelich, P. N. (1989). A simple method for the rapid determination of biogenic opal in pelagic marine sediments. *Deep. Res. (Part I Oceanogr. Res. Pap.* 36, 1415–1426. doi: 10.1016/0198-0149(89)90092-7

Müller, P. J., and Schneider, R. (1993). An automated leaching method for the determination of opal in sediments and particulate matter. *Deep. Res. Part I Oceanogr. Res. Pap.* 40, 425–444. doi: 10.1016/0967-0637(93)90140-X

Murillo, F. J., Kenchington, E., Lawson, J. M., Li, G., and Piper, D. J. W. (2016). Ancient deep-sea sponge grounds on the Flemish cap and grand bank, northwest Atlantic. *Mar. Biol.* 163, 1–11. doi: 10.1007/s00227-016-2839-5

Muscente, A. D., Marc Michel, F., Dale, J. G., and Xiao, S. (2015). Assessing the veracity of precambrian 'sponge' fossils using *in situ* nanoscale analytical techniques. *Precambrian Res.* 263, 142–156. doi: 10.1016/j.precamres.2015.03.010

Nelson, D. M., Tréguer, P., Brzezinski, M. A., Leynaert, A., and Quéguiner, B. (1995). Production and dissolution of biogenic silica in the ocean: revised global estimates, comparison with regional data and relationship to biogenic sedimentation. *Global Biogeochem. Cycles* 9, 359–372. doi: 10.1029/95GB01070

Paasche, E. (1973). Silicon and the ecology of marine plankton diatoms. II. silicate-uptake kinetics in five diatom species. *Mar. Biol.* 19, 262–269. doi: 10.1007/bf02097147

Roubeix, V., Becquevort, S., and Lancelot, C. (2008). Influence of bacteria and salinity on diatom biogenic silica dissolution in estuarine systems. *Biogeochemistry* 88, 47–62. doi: 10.1007/s10533-008-9193-8

Rützler, K., and Macintyre, I. G. (1978). Siliceous sponge spicules in coral reefs sediments. *Mar. Biol.* 49, 147–159. doi: 10.1007/BF00387114

Sim-Smith, C., Ellwood, M., and Kelly, M. (2017). "Sponges as proxies for past climate change events," in *Climate change, ocean acidification and sponges*. Eds. J. C. and J. B. (Berlin: Springer, Cham), 49–78. doi: 10.1007/978-3-319-59008-0_3

Tabachnick, K. R., Menshenina, L. L., Pisera, A., and Ehrlich, H. (2011). Revision of *Aspidoscopulia* reiswig 2002 (Porifera: Hexactinellida: Farreidae) with description of two new species. *Zootaxa* 2883, 1–22. doi: 10.11646/zootaxa.2883.1.1

Talevski, T., Talevska Leshoska, A., Pejoski, E., Pejin, B., Machałowski, T., Wysokowski, M., et al. (2020). Identification and first insights into the structure of chitin from the endemic freshwater demosponge ochridaspongia rotunda (Arndt 1937). *Int. J. Biol. Macromol.* 162, 1187–1194. doi: 10.1016/J.IJBIOMAC.2020.06.247

Tang, Q., Wan, B., Yuan, X., Muscente, A. D., and Xiao, S. (2019). Spiculogenesis and biomineralization in early sponge animals. *Nat. Commun.* 10, 3348. doi: 10.1038/s41467-019-11297-4

Toullec, J., and Moriceau, B. (2018). Transparent exopolymeric particles (TEP) selectively increase biogenic silica dissolution from fossil diatoms as compared to fresh diatoms. *Front. Mar. Sci.* 5. doi: 10.3389/FMARS.2018.00102/BIBTEX

Tréguer, P. J., and de la Rocha, C. L. (2013). The world ocean silica cycle. *Ann. Rev. Mar. Sci.* 5, 477–501. doi: 10.1146/annurev-marine-121211-172346

Tréguer, P. J., Sutton, J. N., Brzezinski, M., Charette, M. A., Devries, T., Dutkiewicz, S., et al. (2021). Reviews and syntheses: The biogeochemical cycle of silicon in the modern ocean. *Biogeosciences* 18, 1269–1289. doi: 10.5194/bg-18-1269-2021

Tsurkan, M. V., Voronkina, A., Khrunyk, Y., Wysokowski, M., Petrenko, I., and Ehrlich, H. (2021). Progress in Chitin Analytics. *Carb. Pol.* 252, 117204. doi: 10.1016/j.carbpol.2020.117204

Van Bennekom, A. J., Buma, A. G. J., and Nolting, R. F. (1991). Dissolved aluminium in the weddell-Scotia confluence and effect of Al on the dissolution kinetics of biogenic silica. *Mar. Chem.* 35, 423–434. doi: 10.1016/S0304-4203(09)90034-2

Van Cappellen, P., Dixit, S., and van Beusekom, J. (2002). Biogenic silica dissolution in the oceans: Reconciling experimental and field-based dissolution rates. *Global Biogeochem. Cycles* 16, 23-1-23–10. doi: 10.1029/2001gb001431